

Prediction of the release process of the nitrogen-extinguishant binary mixture considering surface tension

Siyuan Liu^a, Yongqi Xie^{a*}, Mengdong Chen^b, Jianqin Zhu^{c**}, Rodney Day^d, Hongwei Wu^d, Jianzu Yu^a

^aSchool of Aeronautic Science and Engineering, Beihang University, Beijing, 100191, China

^bGlobal Energy Interconnection Research Institute, Beijing, 102200, China

^cNational Key Laboratory of Science and Technology on Aero-Engines, School of Energy and Power Engineering, Beihang University, Beijing 100191, China

^dSchool of Engineering and Computer Science, University of Hertfordshire, Hatfield, AL10 9AB, United Kingdom

Abstract

Nitrogen used for pressurization in the extinguisher can be partially dissolved in the fire extinguishing agent. Consequently, the evolution of the dissolved nitrogen has a significant effect on the release behavior of the fire extinguishing agent in a rapid process. In this article, a new model was developed to predict the critical pressure of the nitrogen evolution and the release process of the fire extinguishing agent was described in detail. According to the Peng-Robinson (PR) equation of state and van der Waals mixing rule, the effect of the dissolved nitrogen on the surface tension of the fire extinguishant was analyzed by considering surface phase and fugacity coefficient. A method to calculate the surface tension of the liquid agent dissolved with nitrogen was proposed. The results showed that the proposed model can determine the accurate critical pressure of the evolution of the dissolved nitrogen and further evaluated whether nitrogen escapes. At different initial filling pressure, in addition, the release process of the nitrogen-extinguishant such as CF₃I, FC218 (C₃F₈), HFC125 (C₂HF₅), and Halon1301 (CF₃Br) was well predicted by the fluid release model when taking the surface tension and adiabatic index of the mixture into account. Compared with the previously obtained experimental data, the predictions obtained indicated that the present model can adequately describe the liquid and the gas mixture release stage in the release process of the nitrogen-extinguishant.

Keywords: gas-liquid equilibrium; equation of state; surface tension; homogeneous nucleation; escaping pressure; adiabatic index

33 **Nomenclature**

34	A	Cohesive energy parameter in the PR equation of state, Pa m ⁶ mol ⁻²
35	A	Surface area, m ² ; Constant defined in Eq. (9)
36	b	Volumetric parameter in the PR equation of state, m ³ mol ⁻¹
37	B	Constant defined in Eq. (9)
38	f	fugacity, Pa
39	J	Nucleation rate, nuclei cm ⁻³ s ⁻¹
40	k	Binary interaction parameter
41	M	Molecular mass, g
42	N_A	Avogadro constant, 6.02×10 ²³ mol ⁻¹
43	p	Pressure, Pa
44	p_e	Bubble-point pressure, Pa
45	R	Molar gas constant, 8.3145 J mol ⁻¹ K ⁻¹
46	T	Absolute temperature, K
47	T_i	Initial temperature, K
48	v	Molar volume, m ³ /mol
49	x, X	Mole fraction
50	y, Y	Mole fraction
51	Z	Compressibility factor
52	V	Volume, m ³

53 ***Greek letters***

54	α	Function of temperature in the PR equation of state
55	α_{ij}	Binary parameter
56	κ	Function of the acentric factor
57	φ	Fugacity coefficient
58	ω	Acentric factor

59 ***Superscripts***

60	G	Gas
61	L	Liquid

62 ***Subscripts***

63	1	Nitrogen
64	2	Agent
65	B	Bulk phase
66	c	Critical point
67	<i>i, j</i>	Component identification
68	m	Mixture
69	r	Reduced parameter
70	S	Surface phase
71	b	Bottle

72 **1. Introduction**

73 Aircrafts may be confronted with the threat of fire. As an important subsystem of an aircraft,
74 a fire suppression system equipped for an engine cabin can release sufficient fire extinguishing
75 agent to put out a fire to guarantee safety. Nowadays, Halon1301 is normally utilized in military
76 aircrafts since it is nontoxic and effective as fire extinguishing agent [1]. However, Halon1301
77 has been banned from production and utilization under Montreal Protocol which addresses
78 global environmental concerns and the potential of high ozone depletion. Therefore, halon
79 alternatives are being produced and used in recent years [2-4]. Grosshandler et al. [5] adopted
80 CF₃I, FC218 and HFC125 to replace Halon1301 for the fire suppression in the dry bay. Saso et
81 al. [6] examined the fire suppression effects of three kinds of hydrofluorocarbons (HFC) and
82 perfluorocarbon (FC). Generally, these agents have low saturation vapor pressure at room
83 temperature. In order to speed up the release of the agent, nitrogen is practically used as the
84 pressurized medium in the extinguisher, which can ensure that the pressure is high enough inside
85 the bottle when extinguishing fire at low temperature. Two typical filling pressures of 2.5 MPa
86 and 4.2 MPa are always applied.

87 For the different initial filling pressure in the bottle, the pressure decay curve shows an
88 obvious difference in the process of releasing Halon1301 [7-9]. For a low filling pressure,
89 nitrogen dissolved in the liquid agent cannot escape in the process of the releasing extinguishing
90 agent. Under this condition, the release process was approximately divided into two stages by
91 Elliott [7] and Yang [8, 9]. However, when the filling pressure is high, the nitrogen dissolved in
92 the liquid agent will come out of the liquid along with a rapid pressure drop in the bottle, which

93 has been verified by the rapid release test of agent. As the total pressure in bottle is lower than
94 the nucleation pressure of the dissolved nitrogen, the nitrogen is released in the form of bubbles
95 from the liquid agent. This will lead to the short-term increase of the pressure in the bottle.
96 Typical pressure-time curves during the low-pressure release and high-pressure release were
97 presented by Yang et al. [9].

98 Experimental investigation on the pressure variation during the release of Halon1301 was
99 performed by Elliott et al. [7], when the initial filling pressure was varied from 4.48 MPa to
100 10.24 MPa and the initial filling temperature was increased from 12 °C to 63 °C, accordingly.
101 However, the critical pressure of the nitrogen evolution was not addressed theoretically. It was
102 only assumed that the total pressure in the escaping bubble was the same as the filling pressure
103 and decreased slowly with the drop of the temperature. Moreover, they also believed that the
104 surface tension of Halon1301 had an important effect on the nitrogen escaping pressure. But
105 they did not take the effect of the dissolved nitrogen on the surface tension of Halon1301 into
106 account.

107 During the release of the extinguishing agent, the dissolved nitrogen may escape and lead
108 to the pressure rise inside the bottle. Elliot et al. [7] studied the Halon1301 release process and
109 assumed that the critical radius of nitrogen escaping bubble was 7.5nm, which has been adopted
110 by HFLOW software. According to the homogeneous nucleation theory, Blander et al. [10] and
111 Forest et al. [11] developed a mathematical model describing the homogeneous nucleation
112 process of bubble in solution. They further validated the model against the experiments for
113 nitrogen dissolved in aether. Yang et al. [9] developed a model to calculate the critical pressure
114 of the nitrogen escape for Halon1301, HFC125, FC218 and CF₃I, which can accurately
115 determine whether nitrogen escape occurs during the release of agent. However, their model can
116 only be used to qualitatively explain the variation of nitrogen escaping pressure. In recent years,
117 some researchers [12,13] calculated the critical bubble size in the process of gas-phase in binary
118 systems through the modified Gibbs' approach, which provided new insights for analyzing the
119 critical radius of the nitrogen escaping bubbles.

120 The determination of the surface tension of the mixture of dissolved nitrogen and liquid agent
121 is involved in the study of the critical state of nitrogen escaping. As for the calculation of the
122 surface tension for pure liquid agent, the method based on the principle of corresponding state
123 and parachor was recognized as the most accurate. For instance, Jiang et al. [14] used a
124 piecewise function method to define the surface tension of the liquid CO₂ based on the Parachor

125 Macleod–Sugden correlation and Brock-Bird correlation. Duan et al. [15] developed a
126 prediction method of surface tension for twenty types of HFCs and HCFCs based on the
127 principle of corresponding state. Nicola and Moglie [16, 17] also presented a similar prediction
128 method for the surface tension of total 28 refrigerants with that developed by Duan et al. [15],
129 such as HFC 227ea, FC218, HFC125 and Halon1301. If combined with a suitable mixing rule,
130 van der Waals equation could also be used to calculate the surface tension of multicomponent
131 HFCs mixtures [18, 19]. Additionally, Carey et al. [20] firstly combined the density gradient
132 theory with the cubic equation of state to determine the surface tension of pure fluid, which
133 expanded the application scope of density gradient theory [21, 22]. In terms of the measurement
134 of the surface tension, recently, Wang [23] studied the surface tension of the organosilicone
135 surfactant as foam extinguishing agent by orthogonal experiments, while Baidakov et al. [24-
136 26] tested the surface tension of the mixed solutions of nitrogen-methane, nitrogen-ethane and
137 methane-ethane in the temperature ranging from 95 K to 170 K, 93 K to 283 K and 93 K to 283
138 K, respectively.

139 Dinunno et al. [27] and Yang et al. [3, 28] proposed mathematical models to analyze the
140 release process of the fire extinguishing agent in bottles. The former assumed that the average
141 release flow in any time step was consistent with the flow when the fluid in the fire extinguisher
142 was stable; while the latter assumed that the gas mixture drove the liquid fire extinguishing agent
143 like a piston during the release process as an adiabatic reversible isentropic process, ignoring
144 the effect of the extinguishing agent vapor.

145 It is significant to accurately determine the specific heat capacity at constant pressure in the
146 calculation of the adiabatic index of actual gas mixture. The thermodynamic properties of fluids
147 can be calculated according to the Maxwell function and the cofunction method. Lemmon and
148 Jacobsen [29, 30] calculated the thermodynamic properties including specific heat capacity at
149 constant pressure of various refrigerants and their mixtures based on Helmholtz free energy
150 equation, but the coefficients of the equation were too many to be convenient to use. He et al.
151 [31] chose PR equation combined with van der Waals mixing rule and 81 M-H equation
152 combined with constant mixing rule to establish a calculation model which can accurately
153 predict the specific heat capacity at constant pressure of pure HFC227ea and pure HFC125.

154 To the best of author's knowledge, there are no detailed researches available in the open

155 literature regarding the effect of the dissolved nitrogen on the surface tension of the liquid fire
156 extinguishing agent and the mathematic model predicting the critical pressure for the evolution
157 of dissolved nitrogen. Therefore, the current work aims to develop a method to calculate the
158 surface tension of the liquid agent dissolved with nitrogen, and further describe the release
159 process of the mixture of nitrogen and fire extinguishing agent. PR equation of state and van der
160 Waals mixing rule are selected and the effect of the dissolved nitrogen on the surface tension of
161 liquid extinguishing agent taking Halon1301 as an example is analyzed and discussed based on
162 the corresponding thermodynamic model. Another major contribution of the current work is to
163 develop a fluid release model in order to predict the release process of the mixture of nitrogen
164 and fire extinguishing agent, such as CF₃I, FC218 (C₃F₈), HFC125 (C₂HF₅), and Halon1301
165 (CF₃Br). The homogeneous nucleation theory is used and a constant critical radius of nitrogen
166 evolution under different filling conditions is assumed, to determine the critical pressure of the
167 nitrogen evolution in the fire extinguisher. Furthermore, based on the state equation and mixing
168 rules, the adiabatic index of the mixture of nitrogen and fire extinguishing agent steam are
169 calculated accurately. According to the actual adiabatic isentropic expansion process of gas, the
170 differential equation of the fluid release process in the fire extinguisher is derived. The fourth-
171 order Runge Kutta method is applied to solve the equation, which can predict the whole release
172 process of various mixtures of nitrogen-extinguishant.

173 2. Surface tension of mixture

174 During the release of the fire extinguishing agent, the surface tension of the liquid agent
175 dissolved with nitrogen has an important impact on nitrogen evolution. As the binary system of
176 nitrogen-extinguishant reaches gas-liquid equilibrium, the surface phase occurs between the gas
177 phase and liquid phase. The components inside the surface phase are considered as constant and
178 uniform distribution. Based on the theoretical model of surface tension, the thermodynamic
179 correlation predicting the surface tension of mixture can be obtained by defining the fugacity of
180 surface phase and fugacity coefficient, and considering the relationship, among surface tension,
181 chemical potential and fugacity [32], as described in the equation below.

$$182 \quad \sigma_m = \frac{A_i}{A_i} \sigma_i + \frac{RT}{A_i} \ln \frac{\varphi_{iS} y_{iS}}{\varphi_{iB} y_{iB}} \quad (1)$$

183 where σ_m is the surface tension of the mixture, σ_i is the surface tension of pure component, A_i
 184 is the molar surface area of the i th pure component, \bar{A}_i is the partial molar surface area of
 185 component i relative to mixture, R is the gas constant, T is the temperature, φ is the fugacity
 186 coefficient, y is the mole fraction, the subscript S and B indicate surface phase and bulk phase,
 187 respectively.

188 For the surface tension σ_i of the pure agent, the following correlation in Eq. (2) provided by
 189 Nicola et al. [16, 17] is adopted with a high precision.

$$190 \quad \sigma_i = 0.658 p_c^{0.618} T_c^{0.34} (1 + \omega)^{0.770} (1 - T/T_c)^{1.262} \quad (2)$$

191 where p_c is the critical pressure, T_c is the critical temperature, ω is the acentric factor, T is the
 192 thermodynamic temperature.

193 In order to use Eq. (1) to calculate the surface tension of the mixture, the following two
 194 assumptions are proposed [32].

195 (1) The partial mole surface area of component i is assumed to be equal to the mole surface
 196 area of the pure component i , i.e., $\bar{A}_i = A_i$. Moreover, the surface phase is considered as
 197 monomolecular layer and molecule of each component is regarded as spherical. Consequently,
 198 \bar{A}_i and A_i can be calculated by Eq. (3):

$$199 \quad \bar{A}_i = A_i = \pi \cdot \left(\frac{3}{4\pi}\right)^{2/3} N_A^{1/3} v_{iB}^{2/3} = 1.21 N_A^{1/3} v_{iB}^{2/3} \quad (3)$$

200 where N_A is Avogadro constant, $=6.02 \times 10^{23} \text{ mol}^{-1}$, v_{iB} is the molar volume of liquid phase for
 201 pure component i .

202 (2) Assuming that the correlation of the fugacity coefficient and component for the surface
 203 phase and bulk phase can be described by equation of state and mixing rule. Because the
 204 component y_{iB} and fugacity coefficient φ_{iB} in the bulk phase follow vapor-liquid equilibrium,
 205 they can be calculated by using appropriate equation of state and mixing rule. Thus, they are
 206 regarded as the known constant.

207 In the current study, the PR equation of state was used, which can be expressed as the
 208 following:

$$209 \quad p = \frac{RT}{v-b} - \frac{a}{v(v+b)+b(v-b)} \quad (4)$$

210 where a and b are the function of temperature. According to the critical parameters and reduced
 211 parameters, both variables can be obtained from the following expressions:

$$212 \quad a = a_c \alpha(T_r) = \frac{0.45724R^2T_c^2 \alpha(T_r)}{p_c} \quad (5)$$

$$213 \quad b = \frac{0.07780RT_c}{p_c} \quad (6)$$

$$214 \quad \alpha(T_r) = [1 + \kappa(1 - T_r^{0.5})]^2 \quad (7)$$

$$215 \quad \kappa = 0.3746 + 1.54226\omega - 0.26992\omega^2 \quad (8)$$

216 where T_r is the reduced temperature, κ is the constant characteristic of each component.

217 In general, Eq. (4) is transformed into cubic equation in one variable corresponding to
 218 compressibility factor Z , which can be expressed as [33]:

$$219 \quad Z^3 - (1 - B)Z^2 + (A - 3B^2 - 2B)Z - (AB - B^2 - B^3) = 0 \quad (9)$$

220 where

$$221 \quad A = \frac{ap}{R^2T^2} \quad (10)$$

$$222 \quad B = \frac{bp}{RT} \quad (11)$$

$$223 \quad Z = \frac{pv}{RT} \quad (12)$$

224 In the current work, the one variable mixing rule of van der Waals is used to define the mixture
 225 parameters in Eqs. (9) - (11):

$$226 \quad a_m = \sum_i \sum_j x_i x_j a_{ij} \quad (13)$$

$$227 \quad b_m = \sum_i x_i b_i \quad (14)$$

$$228 \quad a_{ij} = (a_i a_j)^{0.5} (1 - k_{ij}) \quad (15)$$

229 where k_{ij} is the binary interaction parameter. For nitrogen and different extinguishing agents, the
 230 calculation method of the binary interaction parameters was described in Ref. [34].

231 Consequently, the equations predicting the surface tension of mixture are as follows:

232

$$\begin{cases} \sigma_m = \sigma_i + \frac{RT}{A_i} \ln \frac{\varphi_{iS} y_{iS}}{\varphi_{iB} y_{iB}} \\ \sum_{i=1}^2 y_{iS} = 1 \\ \sigma_i = 0.658 p_c^{0.618} T_c^{0.34} (1 + \omega)^{0.770} (1 - T/T_c)^{1.262} \end{cases} \quad (16)$$

233

In Eq. (16), the unknown variables are y_{1S} , y_{2S} and σ_m , respectively. Therefore, these equations

234

group is close and has unique solution, which can be obtained by using Newton iterative method.

235

3. Fluid release model

236

This paper mainly analyzes the critical condition of dissolved nitrogen evolution based on the

237

discharge model proposed by Yang et al. [9], and discusses the effect of different filling pressures

238

on the critical pressure of nitrogen evolution, to predict the release process of nitrogen-

239

extinguishant.

240

It is assumed that the liquid fire extinguishing agent is clean other than the dissolved nitrogen.

241

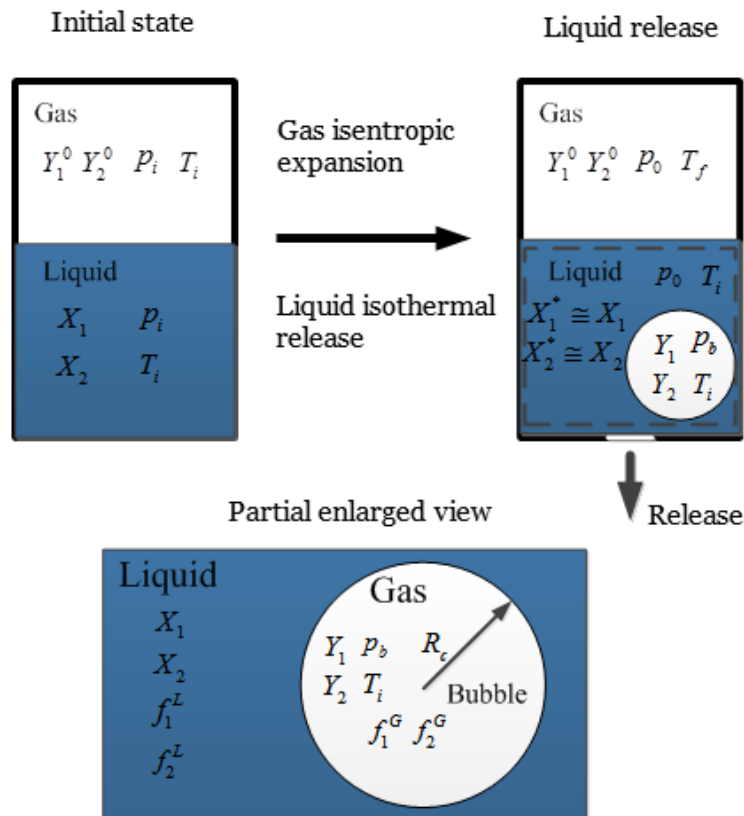
The release of the agent is a rapidly depressurized process. Meanwhile, the liquid phase can be

242

considered as experiencing an isothermal release process. The evolution of dissolved nitrogen

243

is schematically illustrated in Fig. 1, where the size of the gas bubble is exaggerated.



244

245 **Fig. 1 The schematic diagram of release process [9]**

246 When the critical bubbles appear, the unstable thermodynamic equilibrium reaches between
247 the bubbles and surrounding superheated liquid. According to the theory of gas-liquid
248 equilibrium, the fugacity is equal for nitrogen (denoted by '1' in Fig. 1) and fire extinguish agent
249 (denoted by '2' in Fig. 1), as shown by the formula below.

250
$$f_1^L(p_0, T_i, X_1) = f_1^G(p_b, T_i, Y_1) \quad (17)$$

251
$$f_2^L(p_0, T_i, X_2) = f_2^G(p_b, T_i, Y_2) \quad (18)$$

252 where X_1 and X_2 are the mole fractions of nitrogen and extinguishing agent in liquid phase,
253 respectively; Y_1 and Y_2 are the mole fractions of nitrogen and agent vapor in vapor phase,
254 respectively; f_1^G and f_2^G are the fugacity for nitrogen and agent vapor in vapor phase,
255 respectively; f_1^L and f_2^L are the fugacity for nitrogen and agent in liquid phase, respectively;
256 P_0 is the liquid pressure outside bubble; P_b is the pressure inside bubble.

257 The pressure at the interface of bubble and liquid agent should meet the Yang-Laplace
258 equation:

259
$$p_b - p_0 = \frac{2\sigma_m}{R_c} \quad (19)$$

260 where R_c is the critical radius of bubble.

261 It can be seen from Eq. (8) to (10) that there are four unknown variables in total, namely P_b ,
262 P_0 , Y_1 and R_c . One more equation needs to be supplemented to achieve a solution. Referring to
263 the theory of superheat limit kinetics of binary mixture proposed by Holden and Katz [35], Yang
264 et al. [9] added an equation regarding the nucleation rates J , in the form as below:

265
$$J = \frac{N_A}{v^L} \left(\frac{Y_1}{\sqrt{M_1}} + \frac{Y_2}{\sqrt{M_2}} \right) \left(\frac{2\sigma}{\pi} \right)^{0.5} \exp\left(-\frac{4\pi\sigma R_c^2}{3kT_i} \right) \quad (20)$$

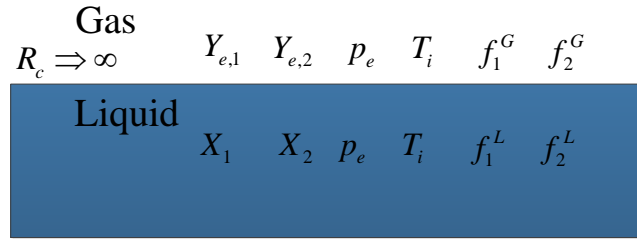
266 where M_1 and M_2 are the molecular masses of the nitrogen and agent, respectively.

267 The results from Yang et al. [9] show that the calculated nitrogen escaping pressure is
268 remarkably lower than the experimental data, although their model shown as Eq. (17) - (20) can
269 accurately determine whether nitrogen gas has escaped during the release of fire extinguishing
270 agent. Therefore, it can only be used to describe the changing trend of nitrogen escaping pressure.
271 In view of this, Eq. (20) is not used as a supplementary equation in the current work, but the

272 critical radius of escaping nitrogen bubble (R_c) under different initial conditions is directly
 273 assumed to be constant.

274 In order to solve the unknown variables in the equation, the scenario of the critical radius of
 275 nitrogen bubble approaching infinity is first analyzed.

276 As the critical radius tends to infinity, the thermodynamic equilibrium for the fluids on both
 277 sides of the bubble is shown in Fig. 2. Where, P_e and T_i are the bubble-point pressure and
 278 temperature, respectively, when the gas-liquid equilibrium is reached.



279
 280 **Fig. 2 The thermodynamic equilibrium at gas-liquid interface for infinite bubble**
 281 **radius**

282 From the theory of gas-liquid phase equilibrium [36, 37], the fugacity of nitrogen and agent
 283 are equal at both sides of the bubble.

$$284 \quad [f_2^L(p_e, T_i, X_2)]_{R_c \rightarrow \infty} = [f_2^G(p_e, T_i, Y_{e,2})]_{R_c \rightarrow \infty} \quad (21)$$

$$285 \quad [f_1^L(p_e, T_i, X_1)]_{R_c \rightarrow \infty} = [f_1^G(p_e, T_i, Y_{e,1})]_{R_c \rightarrow \infty} \quad (22)$$

286 According to the thermodynamic theory, the fugacity for nitrogen and agent can be defined
 287 by Eq. (22).

$$288 \quad \left[\frac{\partial \ln f_i}{\partial p} \right]_{T_i} = \frac{\bar{v}_i}{RT_i} \quad (23)$$

289 Integrate the equation above:

$$290 \quad RT_i \int_{[f_2^L]_{R_c \rightarrow \infty}}^{f_2^L} d \ln f_2^L = \int_{p_e}^{p_0} \bar{v}_2^L dp \quad (24)$$

291 If assuming the partial molar volume of the liquid agent is only a function of temperature,
 292 and slightly affected by pressure and composition, then the above integral turns into:

$$293 \quad f_2^L = [f_2^L]_{R_c \rightarrow \infty} \exp\left[\frac{\bar{v}_2^L (p_0 - p_e)}{RT_i} \right] \quad (25)$$

294 Substituting Eq. (18) and Eq. (21) into the Eq. (25) can obtain:

295
$$f_2^G = [f_2^G]_{R_c \rightarrow \infty} \exp\left[\frac{\bar{v}_2^L (p_0 - p_e)}{RT_i}\right] \quad (26)$$

296 Simultaneously, f_2^G and $[f_2^G]_{R_c \rightarrow \infty}$ is approximately proportional to the partial pressures
 297 under their corresponding conditions, namely:

298
$$\frac{f_2^G}{[f_2^G]_{R_c \rightarrow \infty}} \approx \frac{Y_2 p_b}{Y_{e,2} p_e} \quad (27)$$

299 where, $Y_2 p_b$ and $Y_{e,2} p_e$ represents partial pressure for the agent vapor.

300 Substituting Eq. (18) into Eq. (17) yields:

301
$$Y_2 p_b = Y_{e,2} p_e \exp\left[\frac{\bar{v}_2^L (p_0 - p_e)}{RT_i}\right] \quad (28)$$

302 Employing the procedure like the one described above, a formula to calculate the partial
 303 pressure of nitrogen in the nucleating bubble can be obtained:

304
$$Y_1 p_b = Y_{e,1} p_e \exp\left[\frac{\bar{v}_1^L (p_0 - p_e)}{RT_i}\right] \quad (29)$$

305 In the current study, the PR equation of state and van der Waals mixing rule are chosen to
 306 calculate the partial molar volume for the dissolved nitrogen and liquid agent. The formulas are
 307 as follow:

308
$$\bar{v}_2^L = \frac{RT}{p} \left[Z + X_1 \left(\frac{\partial Z}{\partial X_2} \right)_{T,P} \right] \quad (30)$$

309
$$\bar{v}_1^L = \frac{RT}{p} \left[Z - X_2 \left(\frac{\partial Z}{\partial X_2} \right)_{T,P} \right] \quad (31)$$

310 Using the implicit function derivation rule, $\left(\frac{\partial Z}{\partial X_2} \right)_{T,P}$ can be calculated as the process below:

311
$$\left(\frac{\partial Z}{\partial X_2} \right)_{T,P} = \frac{[-Z^2 + 2Z(1+3B) + A - 2B - 6B^2] \left(\frac{\partial B}{\partial X_2} \right)_{T,P}}{3Z^2 - 2(1-B)Z + (A - 3B^2 - B^3)} + \frac{(B-Z) \left(\frac{\partial A}{\partial X_2} \right)_{T,P}}{3Z^2 - 2(1-B)Z + (A - 3B^2 - B^3)}$$

312 (32)

313 where,

314
$$\left(\frac{\partial A}{\partial X_2} \right)_{T,P} = \frac{p}{R^2 T^2} [2a_{22} X_2 - 2a_{11} X_1 + 2(1 - 2X_2)(1 - k_{12}) \sqrt{a_{11} a_{22}}], \quad \left(\frac{\partial B}{\partial X_2} \right)_{T,P} = \frac{p}{RT} [b_{22} - b_{11}]$$

315 When the bubble radius approaching infinity ($R_c \rightarrow \infty$), and the liquid temperature (T_i) and
316 the mole fraction (X_2) of liquid phase agent is given, the pressure and the mole fraction of the
317 agent vapor inside bubble can be obtained via a simple gas-liquid equilibrium calculation using
318 the PR equation and the van der Waals mixing rule. Combining Eq. (28) and (29), the molar
319 fractions for nitrogen (Y_1) and agent vapor (Y_2) in the nucleating bubble can be obtained.

320 Taking the nitrogen evolution during the release of Halon1301 as an example, this study
321 assumes that the critical radii are different constants in this process. Therefore, to evaluate the
322 accuracy of the model proposed by the authors, the critical escaping pressures calculated by
323 different critical radii will be compared with the experimental data.

324 When the evolution of the nitrogen happening and the values of T_i , X_1 , X_2 and R_c are given,
325 the process of calculating the critical pressure within the nucleation bubble (p_b), the pressure of
326 the liquid phase (p_0), and the molar ratio of nitrogen in bubble (Y_1) are as follow:

327 (1) According to the given values T_i , X_1 and X_2 , the values for p_e , $Y_{e,1}$ and $Y_{e,2}$ can be acquired
328 through the bubble point pressure calculation (bubble point pressure calculation refer to Ref.
329 [34]).

330 (2) Calculate the compression factor $Z(p_e, T_i, X_2)$ corresponding to p_e , T_i , and X_2 .

331 (3) Calculate the partial molar volume $\bar{v}_1^L(p_e, T_i, X_1)$ and $\bar{v}_2^L(p_e, T_i, X_2)$, of nitrogen and
332 agent, respectively.

333 (4) Based on $Z(p_e, T_i, X_2)$, p_e and T_i , calculate the molar volume $v^L(p_e, T_i, X_2)$ of liquid mixture.

334 (5) Assume $p_0=1.0$ MPa.

335 (6) Use Eq. (28) and (29) to calculate p_0 , Y_1 , and Y_2 .

336 (7) Calculate the new p_0 through Eq. (19).

337 (8) Compare the calculated p_0 , stop the calculation as meet $|p_0^{\text{new}} - p_0^{\text{old}}| < 0.001$, otherwise go
338 to step 6 for recalculation.

339 Since nitrogen is a type of insoluble gas in all fire extinguishing agents, the gas mixture and
340 liquid fire extinguishing agent in the fire extinguisher still show obvious stratification even
341 under high filling pressure. It is recognized that the release of the liquid fire extinguishing agent
342 can only last tens of milliseconds after the valve is opened. Therefore, it could be assumed that
343 the energy exchange and mass exchange between the gas mixture and the liquid are strictly

344 restricted. Moreover, the release of the liquid fire extinguishing agent can be considered as the
 345 isothermal decompression process, while the gas mixture undergoes the adiabatic reversible
 346 process of actual gas.

347 Yang et al. [8] did not distinguish the type of the fire extinguishing agent and the filling
 348 pressure strictly, and the adiabatic index was taken as 1.4 when analyzing the fluid release
 349 process. However, the mole ratio of Halon1301 vapor in the gas mixture in the fire extinguisher
 350 is 0.49 when the typical filling pressure is 4.2 MPa [38]. As a result, it is necessary to consider
 351 the influence of the nitrogen and fire extinguishing agent vapor simultaneously when developing
 352 the model of the fluid release process in fire extinguisher.

353 According to the differential relation of the thermodynamics, the calculation formula of the
 354 volume adiabatic index k_v and the temperature adiabatic index k_T is as follows:

$$355 \quad k_v = \frac{Z}{Z_p - RZ_T^2 / c_p} \quad (33)$$

$$356 \quad k_T = \frac{1}{1 - RZ_T / c_p} \quad (34)$$

357 where, c_p is the specific heat capacity of the actual gas at constant pressure, J/(mol·K); Z_p and
 358 Z_T are derivative compression factors, and the definition formulas are as follows:

$$359 \quad Z_p = Z - p \left(\frac{\partial Z}{\partial p} \right)_T \quad (35)$$

$$360 \quad Z_T = Z + T \left(\frac{\partial Z}{\partial T} \right)_p \quad (35)$$

361 Since the gas mixture is only composed of nitrogen and extinguishing agent steam, the PR
 362 equation of state and van der Waals mixing rule are selected to calculate the above derivative
 363 compression factor of gas mixture.

364 For gas mixtures, the PR equation is expressed in the form of cubic equation of compression
 365 factor Z as follows:

$$366 \quad Z^3 - (1 - B_m)Z^2 + (A_m - 3B_m^2 - 2B_m)Z - (A_mB_m - B_m^2 - B_m^3) = 0 \quad (36)$$

367 where, $A_m = a_m p / R^2 T^2$; $B_m = b_m p / RT$; $Z = p v_m / RT$.

368 For the cubic equation of the compression factor, the partial derivatives of pressure and
 369 temperature are respectively calculated by implicit differentiation, and then substituted into the

370 equation of the derivative compression factor, finally the calculation formula of the gas mixture's
 371 derivative compression factor can be obtained as follows:

$$372 \quad \left. \frac{\partial A_m}{\partial T} \right|_p = -\frac{p}{R^2 T^3} [a_1 E_1 y_1^2 + y_1 y_2 (1 - k_{12}) \sqrt{a_1 a_2} (E_1 + E_2) + a_2 E_2 y_2^2 + 2a_m] \quad (37)$$

$$373 \quad \left. \frac{\partial B_m}{\partial T} \right|_p = -\frac{B_m}{T} \quad (38)$$

$$374 \quad Z_p = Z - p \left(\frac{\partial Z}{\partial p} \right)_T = Z - \frac{2A_m B_m - 2B_m^2 - 3B_m^3 - Z^2 B_m - Z(A - 6B_m^2 - 2B_m)}{3Z^2 - 2(1 - B_m)Z + (A - 3B_m^2 - B_m^3)} \quad (39)$$

$$\begin{aligned} 375 \quad Z_T &= Z + T \left(\frac{\partial Z}{\partial T} \right)_p \\ &= Z + \frac{B_m Z^2 + [-6B^2 - 2B + p / R^2 T^2 \left(\frac{\partial A_m}{\partial T} \right)_p] Z - Bp / R^2 T^2 \left(\frac{\partial A_m}{\partial T} \right)_p}{3Z^2 - 2(1 - B_m)Z + (A - 3B_m^2 - B_m^3)} \\ &\quad - \frac{A_m B_m + 2B_m^2 + 3B_m^3}{3Z^2 - 2(1 - B_m)Z + (A - 3B_m^2 - B_m^3)} \end{aligned} \quad (40)$$

376 where, $E_1 = k_1 \sqrt{T_{1,r} / \alpha_1}$; $E_2 = k_2 \sqrt{T_{2,r} / \alpha_2}$.

377 In addition, the specific heat capacity $c_{p,m}$ of the mixture of nitrogen and extinguishing agent
 378 steam under pressure can be calculated by the following formula:

$$379 \quad c_{p,m} = \sum_i c_{p,i} y_i \quad (41)$$

380 where, y_i is the mole fraction of each component; $c_{p,i}$ is the specific heat capacity of each
 381 component at constant pressure.

382 Based on the above method of critical pressure of nitrogen and adiabatic index of gas mixture,
 383 the release model of gas mixture of nitrogen and extinguishing agent steam is finally obtained
 384 as follows:

$$385 \quad \frac{dp}{dt} + \frac{pk_v}{V_b} C_d A \sqrt{\frac{2(p - p_a)}{\rho_{l,m}}} = 0 \quad (42)$$

386 where, V_b is the volume of the fire extinguisher; C_d is the liquid emission coefficient, and the
 387 NIST recommended value is 0.61 to 0.64 [8]; A is the cross-sectional area of the small hole; p_a
 388 is the atmospheric ambient pressure.

389 The total pressure in the fire extinguisher at each time step in the above formula can be
 390 calculated by the fourth-order Runge Kutta method [39]. Before the liquid phase at the bottom

391 of the fire extinguisher is released completely, if the pressure in the fire extinguisher is less than
 392 the predicted value of critical pressure of nitrogen evolution, it can be determined that the
 393 nitrogen escapes, and the gas-liquid interface after nitrogen escapes needs to be redefined;
 394 otherwise, the nitrogen will not escape during the whole releasing process.

395 If nitrogen does not escape during the release of the extinguishing agent, the gas mixture will
 396 be filled with the fire extinguisher after the release. Therefore, the subsequent release process
 397 can be treated as an open system. In the current work, the calculation model mentioned in Ref.
 398 [8] can be used:

$$399 \quad \frac{p}{p_{\text{full}}} = \left[1 - \frac{C_A A}{V_b} \left(\frac{RT_{\text{full}} k_V^3 K}{m} \right)^{0.5} \left(\frac{1 - k_V}{2k_V} \right) t \right]^{\frac{2k_V}{1 - k_V}} \quad (43)$$

400 where, $K = [1 / (k_V + 1)]^{(k_V + 1) / (k_V - 1)}$, C_A is the gas emission coefficient, and the value is 0.61; m
 401 is the equivalent molecular mass of the gas mixture which can be calculated according to the
 402 molar components of nitrogen and fire extinguishing agent steam; p_{full} and T_{full} are the pressure
 403 and temperature respectively at the moment when the liquid is released and the gas mixture is
 404 filled with the fire extinguisher.

405 If nitrogen escapes during the release of the liquid extinguishing agent, the volume of the gas
 406 mixture and liquid after nitrogen escapes must be recalculated separately. In the current study,
 407 it is assumed that all the escaping bubbles stay in the liquid layer while the process of the
 408 subsequent bubble growth and rising are ignored. Therefore, the escape of the nitrogen makes
 409 the liquid layer expand upward and the gas phase space decrease correspondingly. If this process
 410 is regarded as isentropic change, the pressure formula of compressed gas phase space is as
 411 follows:

$$412 \quad p' = p_{\text{bd}} \left(\frac{V_{\text{bd}}}{V_{\text{compress}}} \right)^{k_V} \quad (44)$$

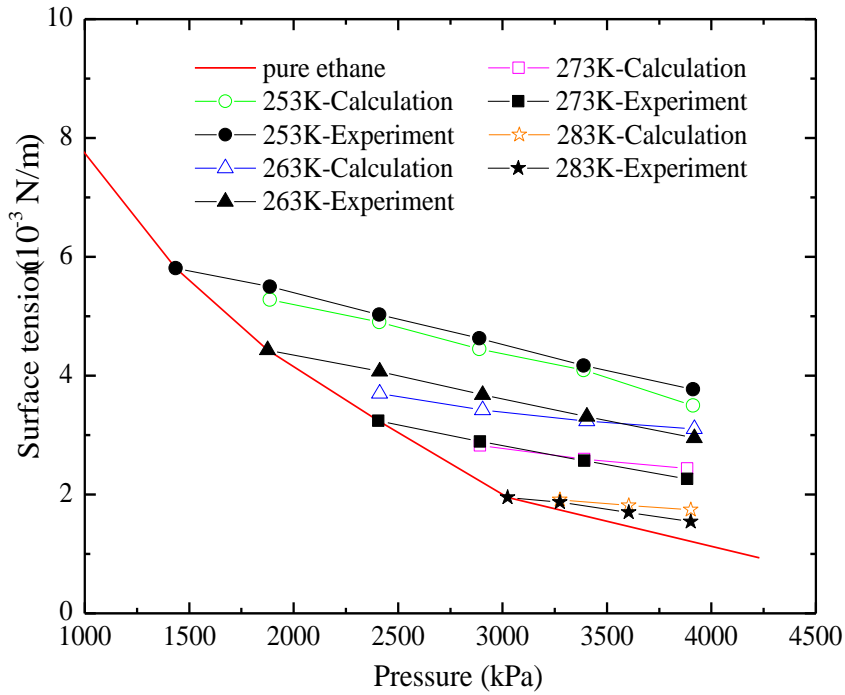
413 where, p_{bd} and V_{bd} are pressure and volume of the gas mixture in the fire extinguisher before
 414 nitrogen escaping respectively.

415 **4. Results and discussion**

416 **4.1 Surface tension of nitrogen-extinguishant mixture**

417 The dissolved nitrogen can change the surface tension of the mixture of fire extinguishing

418 agent and nitrogen. According to the literature review, there is no experimental data regarding
 419 the surface tension of binary mixture of nitrogen and extinguishing agents. To verify the
 420 accuracy of Eq. (16), the surface tension of nitrogen-ethane mixture in Ref. [27] are cited for
 421 evaluation. The temperature range for the selected data is 253 K - 283 K, and the pressure range
 422 is 1.44 MPa - 3.92 MPa. The calculated results are compared to the experimental data in Ref.
 423 [27], as shown in Fig. 3.

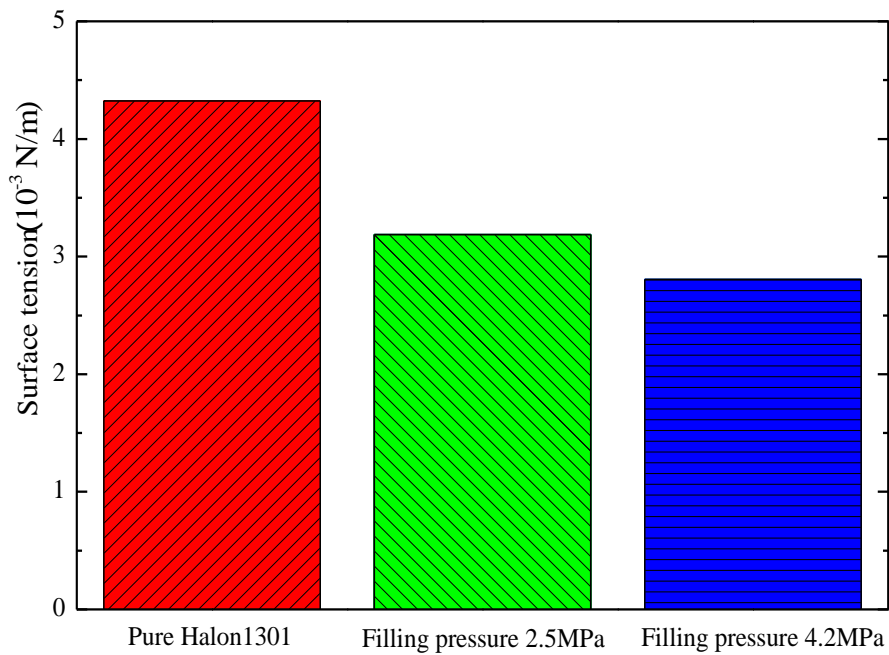


424
 425 **Fig. 3 Comparison between the calculated and experimental data for nitrogen-ethane**
 426 **mixture**

427 Fig. 3 shows that the surface tension of nitrogen-ethane solution decreases with the
 428 temperature and pressure increasing. Compared to the surface tension of pure ethane, the surface
 429 tension of mixture decreases approximately linearly as the amount of dissolved nitrogen
 430 gradually increases. In the range of investigated temperature and pressure, the surface tension
 431 calculated by Eq. (16) is basically consistent with the experimental data, with an average relative
 432 deviation less than 2.8%, which verifies that the model to predict surface tension of mixture is
 433 accurate and effective.

434 Taking Halon1301 as an example, the influence of different filling pressures on the surface
 435 tension of nitrogen- extinguishant mixture is analyzed. The given operating conditions are as
 436 follow: the volume of fire extinguisher is $2.35 \times 10^{-3} \text{ m}^3$, the filling amount of Halon1301 is 1.89
 437 kg, the filling temperature is 293.15 K, and the filling pressure is 2.5 MPa and 4.2 MPa.

438 The calculated results for the surface tension of nitrogen-Halon1301 solution under different
439 filling pressures are shown in Fig. 4. As can be seen from Fig. 4, the surface tension of the
440 mixture gradually decreases with the increase of filling pressure at the same temperature. Given
441 that filling pressure is 4.2 MPa, the surface tension for nitrogen-Halon1301 solution is only 65%
442 of that for pure Halon1301, which means that the absolute difference between the two cases is
443 1.5×10^{-3} N/m. Therefore, the effect of dissolved nitrogen needs to be considered when
444 calculating the escaping pressure of nitrogen during the release of the fire extinguishing agent.



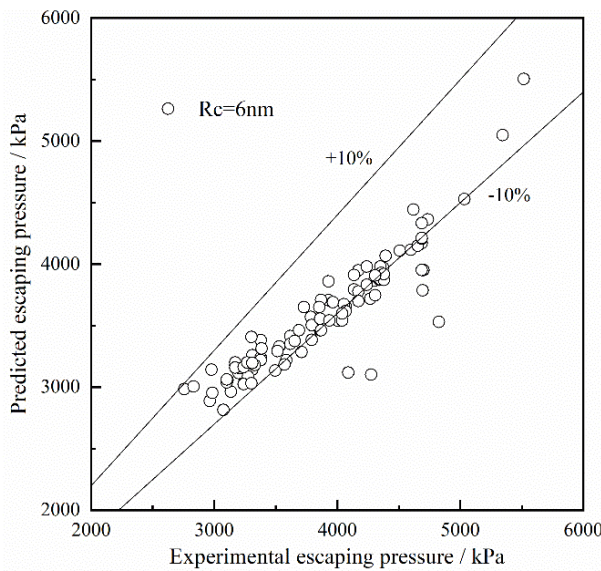
445
446 **Fig. 4 The surface tension of nitrogen-Halon1301 solution under different operating**
447 **conditions**

448 4.2 Critical pressure of nitrogen evolution

449 Some extensive experiments on Halon1301 release were carried out by Elliot et al. [7] and
450 the critical pressures when the evolution of the nitrogen happening were recorded. These provide
451 an experimental evidence for comparing the accuracy of different nitrogen evolution prediction
452 models. When calculating the critical pressure of nitrogen evolution, both Elliot et al. [7] and
453 Yang et al. [9] directly used the equation which calculates the surface tension of pure substance,
454 but ignored the influence of dissolved nitrogen on the surface tension of the agent. However, it
455 has been analyzed in section 4.1 that the dissolved nitrogen has an obvious effect on the surface
456 tension of the agent. Therefore, the equation to calculate surface tension of the nitrogen-
457 extinguishant mixture is employed in this study to calculate the escaping pressure of the nitrogen.

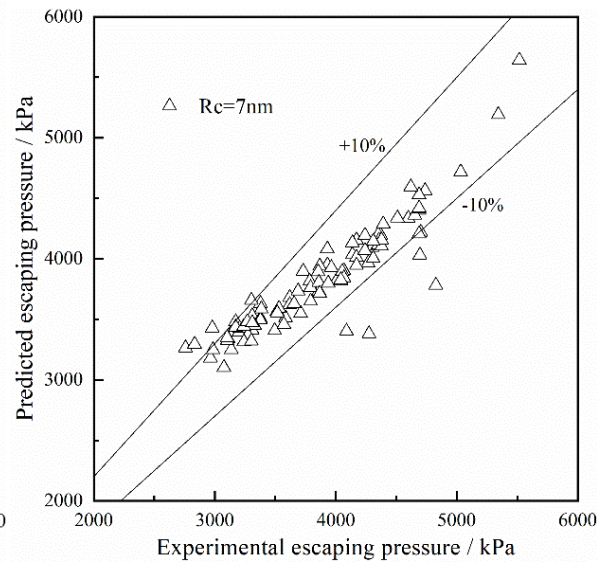
458 When the critical radius is set as 6nm ~ 9nm, the comparison between the predicted and the

459 experimental value of the critical pressure of the nitrogen escaping is presented in Fig. 5. The
 460 surface tension of the mixture of Halon1301 and nitrogen is assumed as that of a pure substance,
 461 which was calculated by Eq. (2). It can be found from Fig. 5 that as the critical pressure of
 462 nitrogen escaping is small (less than 3.5 MPa), the predicted critical pressure is closer to the
 463 experimental value for the critical radius of 6nm. When the critical pressure increases, the value
 464 of the critical radius should be increased to obtain more accuracy results. In general, as the
 465 critical radius is set as 6nm, 7nm, 7.5nm, 8nm and 9nm, the mean relative deviations between
 466 predicted and experimental values for the critical escaping pressure are 8.9%, 5.8%, 6.2%, 7.2%
 467 and 10.0%, respectively. The critical radius between 7nm and 7.5nm is considered as a
 468 reasonable value for all the experimental cases. The result is in a good agreement with the value
 469 of the critical pressure suggested by Elliot et al. [7].



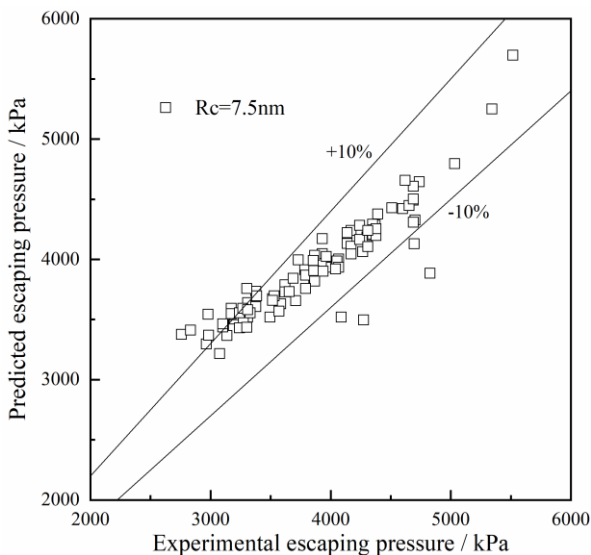
470

(a) Critical radius 6 nm

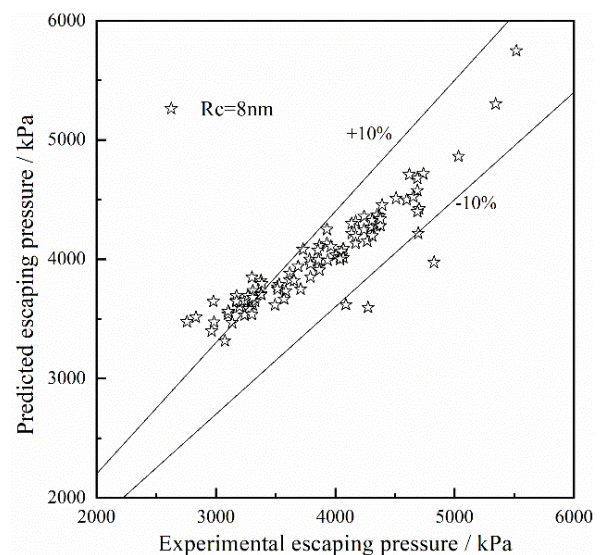


471

(b) Critical radius 7 nm



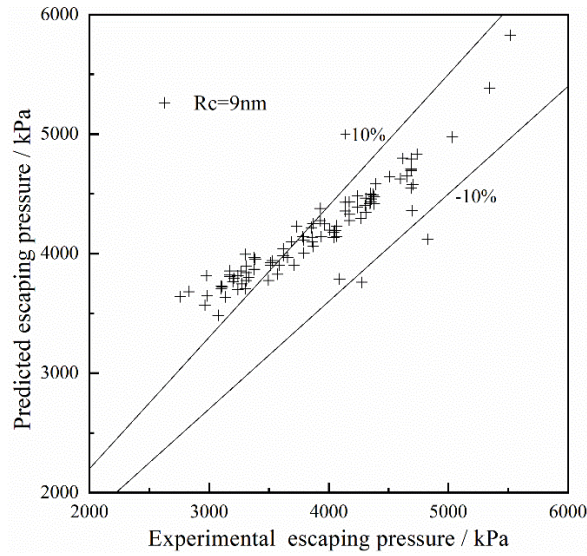
472



473

(c) Critical radius 7.5 nm

(d) Critical radius 8 nm



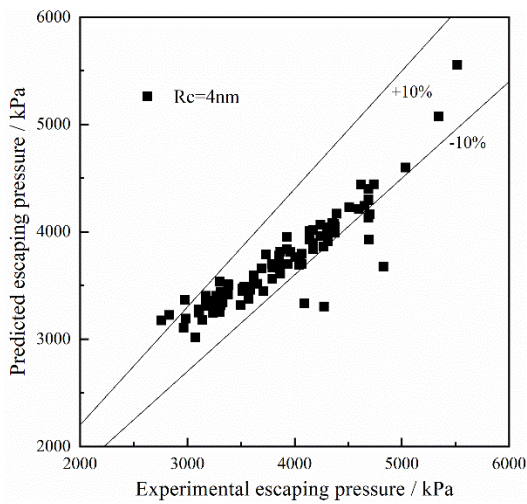
474

475

(e) Critical radius 9 nm

Fig. 5 Comparison between the predicted and experimental value of critical escaping pressure using surface tension of a pure substance

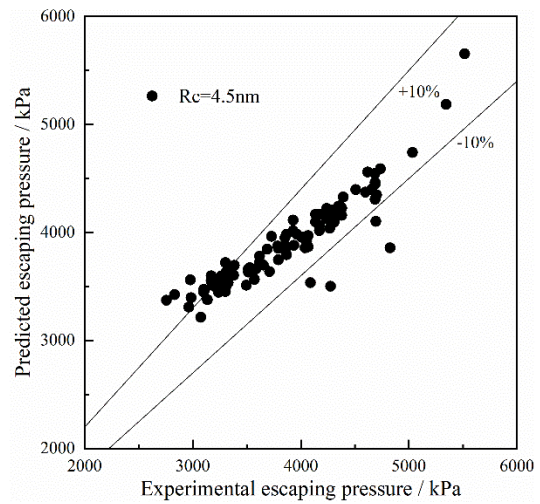
477



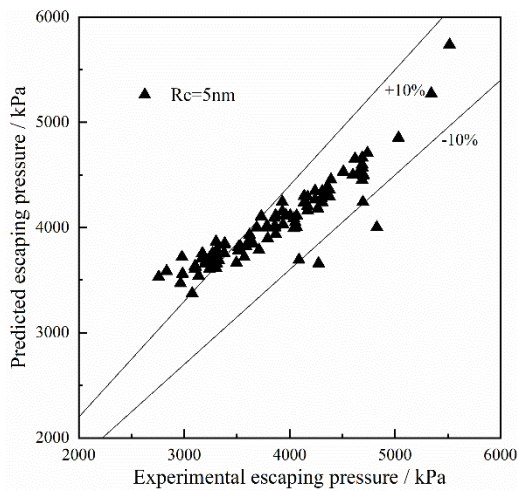
478

479

(a) Critical radius 4 nm



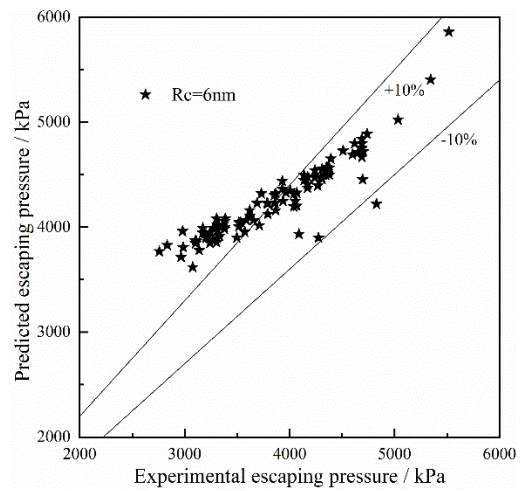
(b) Critical radius 4.5 nm



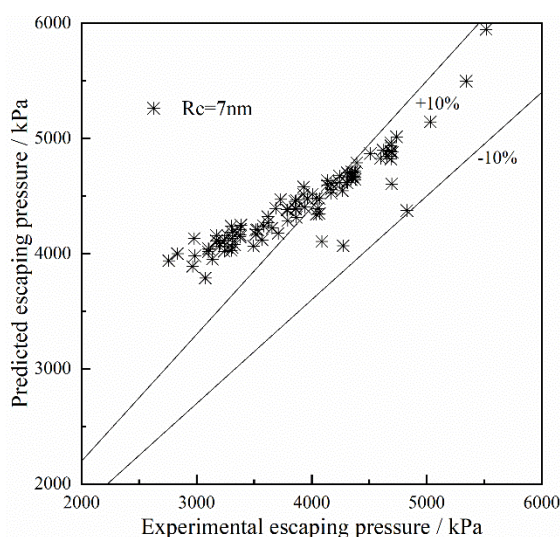
480

481

(c) Critical radius 5 nm



(d) Critical radius 6 nm



(e) Critical radius 7 nm

Fig. 6 Comparison between the predicted and experimental value of critical escaping pressure using surface tension of mixture

482

483

484

485

486 When the critical radius is set as 4nm ~ 7nm, the comparison between the predicted and the
 487 experimental value of the critical escaping pressure of the nitrogen is presented in Fig. 6. It
 488 should be noticed that if using the Eq. (1) to calculate surface tension the critical radius needs
 489 to be increased as the experimental critical escaping pressure of the nitrogen gradually raises.
 490 This can be explained by the Yang-Laplace equation, namely, the surface tension of nitrogen-
 491 Halon1301 mixture is smaller than that of pure Halon1301 under the same conditions. Thus, the
 492 critical radius selected in Yang-Laplace equation also should be smaller. For all the nitrogen
 493 evolution experiments, the average relative deviations between predicted and experimental
 494 values for the critical escaping pressure are 6.4%, 6.5%, 7.9%, 12.4%, and 16.2%, for the critical
 495 radii of 4nm, 4.5nm, 5nm, 6nm and 7nm, respectively. For all the filling conditions, the critical
 496 radius of 4nm is a more preferred.

497 4.3 Nitrogen-extinguishant release process

498 In this section, the fluid release model considering the surface tension of the mixture proposed
 499 in the current study is applied to predict the release process of Halon1301 and three kinds of
 500 halon alternatives at atmospheric pressure after filling with nitrogen to typical pressure. In order
 501 to evaluate the accuracy of the fluid release model, the pressure-time curves of the liquid
 502 extinguishant release and the gas mixture release phase are calculated and compared to the
 503 experimental data in Ref. [8].

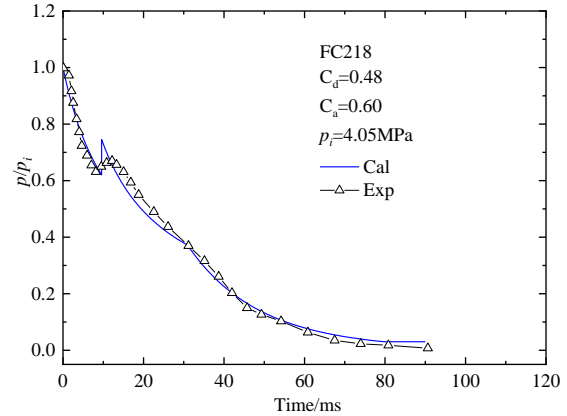
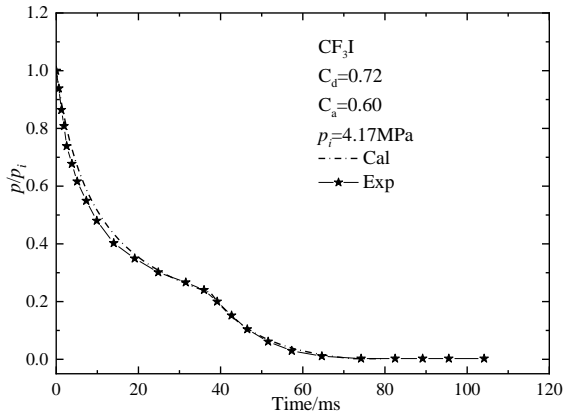
504 The six known conditions of the validation cases are shown in Table 1. In all cases, the

505 equivalent diameters of the valve at the bottom of the fire extinguisher used are 24.5 mm, and
 506 the critical radius of the nitrogen escape are taken as 4 nm. For the mixtures of nitrogen-CF₃I,
 507 nitrogen-FC218, nitrogen-HFC125, and nitrogen-Halon1301 under corresponding operating
 508 condition, the calculated optimum binary interaction parameters are 0.02501, 0.12328, 0.17524
 509 and 0.04920, respectively.

510 **Table 1 The known conditions of the validation cases**

Condition	Type of extinguishant	Quality of extinguishant/kg	Filling pressure/MPa	Ambient temperature/K	Volume of extinguisher /10 ⁻⁴ m ³
I	CF ₃ I	0.755	4.17	294.15	6.10
II	FC218	0.450	4.04	295.15	6.10
III	HFC125	0.438	4.03	294.15	6.10
IV	Halon1301	0.591	4.10	295.15	6.10
V	Halon1301	0.564	4.05	295.15	6.10
VI	Halon1301	0.586	2.75	294.15	6.10

511
 512 The comparison between the predicted value and the experimental data of the release process
 513 of nitrogen-extinguishant under six different operating conditions is shown in Fig. 7, where the
 514 gauge pressure in the bottle has been converted into dimensionless pressure p/p_i , and Fig. 7 (a)
 515 to (f) correspond to the calculation results of conditions I to VI. Based on the fluid release model
 516 proposed in the current study, the critical pressures of the nitrogen escape under the six operating
 517 conditions are 0.94 MPa, 2.58 MPa, 2.41 MPa, 2.53 MPa, 2.49 MPa, and 1.23 MPa, and the
 518 volume adiabatic indexes are 1.41, 1.16, 1.19, 1.233, 1.229, and 1.127, respectively. Under
 519 conditions I and VI, the dissolved nitrogen does not escape, and the mixture release process
 520 clearly presents two stages: the liquid extinguishant release stage and the gas mixture release
 521 stage. However, the evolution phenomenon of the dissolved nitrogen occurs in the cases under
 522 conditions II to V in Fig. 7 due to the high filling pressure, accompanied by the transient increase
 523 of pressure in the fire extinguisher. The whole fluid release process presents four stages: 1) The
 524 superheated liquid release stage, accompanied by the decrease of pressure; 2) The nitrogen
 525 escaping stage, accompanied by the increase of pressure in the bottle; 3) The release stage of
 526 the two-phase fluid consisting of the escape bubble and liquid extinguishant; 4) The gas mixture
 527 release stage.

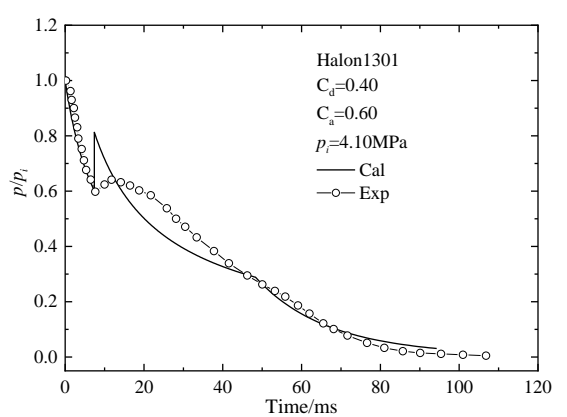
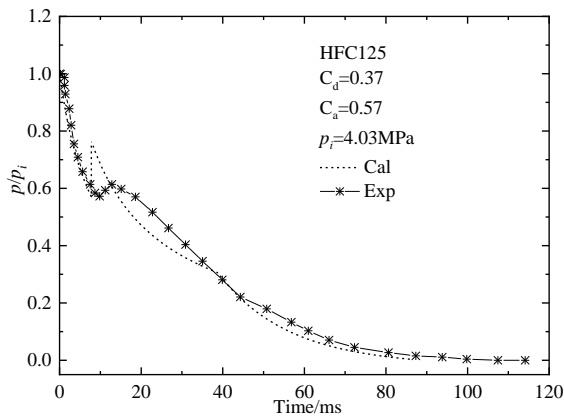


528

529

(a) Condition I

(b) Condition II

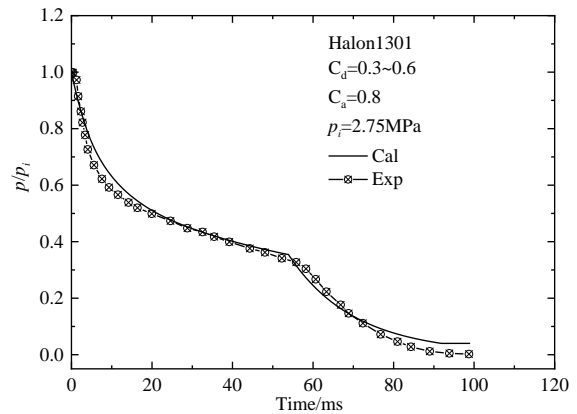
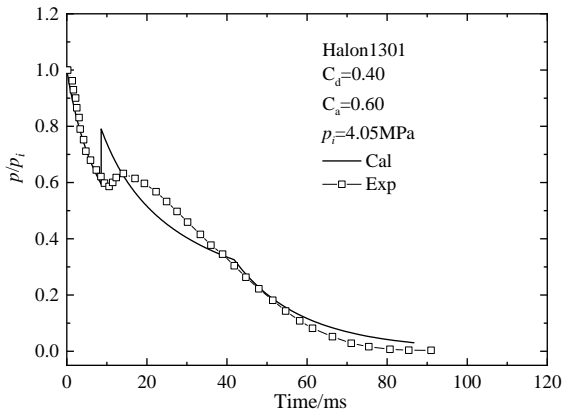


530

531

(c) Condition III

(d) Condition IV



532

533

534

535

536

537

538

539

(e) Condition V

(f) Condition VI

Fig. 7 Comparison between predicted and experimental value of nitrogen-extinguishant release process

According to the experimental data, the nitrogen escaping pressures under conditions II to V are about 2.66 MPa, 2.30 MPa, 2.51 MPa, and 2.43 MPa, and the corresponding average relative deviations between predicted value and experimental data are 3.0%, 4.8%, 0.8% and 2.5%, respectively. Due to the neglect of the growth and rise process of the nitrogen bubble, the

540 predicted pressures in the fire extinguisher during the release stage of two-phase flow are greater
541 than the experimental data under conditions II to V, while the prediction results of other stages
542 and conditions are in good agreement with the experimental data. Taking condition II as an
543 example, the average relative deviation between the calculated and the experimental pressure in
544 the liquid and two-phase fluid release stages is about 5.8%, and that in the nitrogen-FC218 steam
545 mixture release stage is about 4.7%. In addition, the predicted and experimental gas mixtures
546 are filled with the fire extinguisher at 32 ms and 35 ms respectively, with a difference of about
547 3 ms.

548 Moreover, it is believed that the release model can be used to predict the other nitrogen-
549 extinguishant mixtures. In addition, it would be better that the verification is performed if the
550 corresponding experimental data can be provided.

551 Therefore, it can be considered that the proposed release model can accurately predict the
552 release process of multiple binary mixtures of nitrogen and fire extinguishing agent and
553 calculate the change of pressure in the fire extinguisher with time.

554 **5. Conclusions**

555 According to PR equation of state and van der Waals mixing rule, this article calculates the
556 surface tension of the fire extinguishing agent dissolved nitrogen based on the thermodynamic
557 model. The results show that the surface tension of the liquid agent decreased obviously after it
558 dissolved with nitrogen. Consequently, a prediction model of the critical escaping pressure of
559 dissolved nitrogen during the release of fire extinguishing agent is developed based on the
560 homogeneous nucleation theory. The critical radius value of nitrogen evolution is discussed.
561 Comparing to critical pressure of nitrogen evolution reported in a large amount of Halon 1301
562 release experiments from literature, the results indicate that the average relative deviation
563 between the predicted and experimental critical escaping pressure is approximate 6.4% when
564 the critical radius of nitrogen evolution is 4 nm. The prediction model can not only accurately
565 determine whether the dissolved nitrogen evolution occur, but also calculate the critical escaping
566 pressure of dissolved nitrogen more accurately. Moreover, an improved fluid release model is
567 developed to predict the release process of various nitrogen-extinguishant binary systems, such
568 as nitrogen-CF₃I, nitrogen-FC218, nitrogen-HFC125, and nitrogen-Halon1301. In comparison
569 with the previous experimental data, the pressure-time curves in the liquid and the gas mixture
570 release stage can be described well by the fluid release model.

571 **References**

- 572 [1] Takahashi F, Katta VR, Linteris GT, Babushok VI. A computational study of extinguishment
573 and enhancement of propane cup-burner flames by halon and alternative agents. *Fire Saf J.*
574 2017; 91: 688-694.
- 575 [2] Zhang T, Liu H, Han Z, Wang Y, Guo Z, Wang C. Experimental study on the synergistic
576 effect of fire extinguishing by water and potassium salts. *J Therm Anal Calorim.* 2019; 138:
577 857–867.
- 578 [3] Gann RG. Guidance for advanced fire suppression in aircraft. *Fire Technol.* 2008; 44(3):
579 263-282.
- 580 [4] Hodgs SE, McCormick SJ. Fire extinguishing agents for protection of occupied spaces in
581 military ground vehicles. *Fire Technol.* 2013; 49(2): 379-394.
- 582 [5] Grosshandler WL, Gann RG, Pitts WM. Evaluation of alternative in-flight fire suppressants
583 for full-scale testing in simulated aircraft engine nacelles and dry bays. NIST SP-861,
584 Washington DC; 1994.
- 585 [6] Saso Y, Saito N, Liao C, Ogawa Y. Extinction of counterflow diffusion flames with halon
586 replacements. *Fire Saf J.* 1996; 26(4): 303-326.
- 587 [7] Elliott DG, Garrison PW, Klein GA, Moran KM, Zydowicz M P. Flow of nitrogen
588 pressurized halon 1301 in fire extinguishing Systems. JPL Publication 84-62, Jet Propulsion
589 Laboratory; 1984.
- 590 [8] Yang JC, Cleary TG, Vázquez I, Boyer CI, King MD, Breuel BD, Gmurczyk G.
591 Optimization of system discharge. In: *Fire suppression system performance of alternative*
592 *agents in aircraft engine and dry bay laboratory simulations*, NIST SP-890, Washington DC,
593 1995. pp 407-782.
- 594 [9] Yang JC, Cleary TG, Huber ML, Grosshandler WL. Vapour nucleation in a cryogenic- fluid-
595 dissolved-nitrogen mixture during rapid depressurization. *The Royal Society.* 1999; 455:
596 1717-1738.
- 597 [10] Blander M, Katz JL. Bubble nucleation in liquids. *AIChE J.* 1975; 21(5): 833-848.
- 598 [11] Forest TW, Ward CA. Homogeneous nucleation of bubbles in solutions at pressures above
599 the vapor pressure of the pure liquid. *J Chem Phys.* 1978; 69(5): 2221-2230.
- 600 [12] Schmelzer WP, Baidakov G, Boltachev S. Kinetics of boiling in binary liquid-gas solutions:

601 comparison of different approaches. *J Chem Phys.*2003; 119(12): 6166-6183.

602 [13]Němec T. Homogeneous bubble nucleation in binary systems of liquid solvent and
603 dissolved gas. *Chem Phys.* 2016; 467: 26-37.

604 [14]Jiang W, Bian J, Liu Y, Gao S, Chen M, Du S. Modification of the CO₂ surface tension
605 calculation model under low-temperature and high-pressure condition. *J Dispersion Sci
606 Technol.* 2017; 38(5): 671-676.

607 [15]Duan Y, Zhang C, Lin H, Zhu M. The prediction of surface tension for HFCs and HCFCs.
608 *J Eng Thermophys.* 2001; 22(3): 278-280 (in Chinese).

609 [16]Nicola GD, Moglie M. A generalized equation for the surface tension of refrigerants.
610 *International Journal of Refrigeration.* 2011; 34(4): 1098-1108.

611 [17]Nicola GD, Nicola CD, Moglie M. A new surface tension equation for refrigerants. *Int J
612 Thermophys.* 2013; 34(12): 2243-2260.

613 [18]Zhu J, Duan Y, Yang Z, Lin H. Factors influencing the surface tension of binary hydrocarbon
614 mixtures. *Fuel.* 2014; 116(1):116-122.

615 [19]Duan W, Zhao X, Zeng X, Liu Y. Surface tension of HFC-161 and compressor oil mixtures.
616 *International Journal of Refrigeration.* 2018; 85: 191-199.

617 [20]Carey BS, Scriven LE, Davis HT. Semiempirical theory of surface tensions of pure normal
618 alkanes and alcohols. *AIChE J.* 1978; 24(6): 1076-1080.

619 [21]Liang X, Michelsen ML, Kontogeorgis GM. A density gradient theory based method for
620 surface tension calculations. *Fluid Phase Equilib.* 2016; 428: 153-163.

621 [22]Mu X, Frank F, Alpak FO, Chapman WG. Stabilized density gradient theory algorithm for
622 modeling interfacial properties of pure and mixed systems. *Fluid Phase Equilib.* 2017; 435:
623 118-130.

624 [23]Wang P. Application of green surfactants developing environment friendly foam
625 extinguishing agent. *Fire Technol.* 2015; 51(3): 503-511.

626 [24]Baidakov VG, Khotienkova MN, Andbaeva VN, Kaverin AM. Capillary constant and
627 surface tension of methane-nitrogen solutions: 1. Experiment. *Fluid Phase Equilib.* 2011;
628 301(1): 67-72.

629 [25]Baidakov VG, Kaverin AM, Khotienkova MN, Andbaeva VN. Surface tension of an ethane-
630 nitrogen solution. 1: Experiment and thermodynamic analysis of the results. *Fluid Phase*

631 Equilib. 2012; 328(35): 13-20.

632 [26]Baidakov VG, Kaverin AM, Khotienkova MN. Surface tension of ethane-methane solutions:
633 1. Experiment and thermodynamic analysis of the results. Fluid Phase Equilib. 2013;
634 356(10): 90-95.

635 [27]Dinenno PJ, Hanauska CP, Forssell EW. Design and engineering aspects of halon
636 replacements. Process Saf Prog. 1995; 14(1): 57-62.

637 [28]Yang JC, Pitts WM, Breuel BD, Grosshandler WL, Cleveland WG. Rapid discharge of a
638 fire suppressing agent. Int Commun Heat Mass Transf. 1996; 23(23): 835–844.

639 [29]Lemmon EW, Jacobsen RT. A generalized model for the thermodynamic properties of
640 mixtures. Int J Thermophys. 1999; 20(3): 825-835.

641 [30]Lemmon EW, Jacobsen RT. Thermodynamic properties of mixtures of R-32, R-125, R-134a,
642 and R-152a. Int J Thermophys. 1999; 20(6): 1629-1638.

643 [31]He MG, Yang YJ, Zhang Y, Zhang XX. Theoretical estimation of the isobaric heat capacity
644 c_p of refrigerant. Appl Therm Eng. 2008; 28(14): 1813-1825.

645 [32]Hu YQ, Li ZB, Lu JF, Li YG, Jin Y. Surface tension calculation of liquid mixtures by PR
646 EOS. Chem Eng (in Chinese). 1997; 25(3): 42-45.

647 [33]Peng DY, Robinson DB. A new two-constant equation of state. Industrial and Engineering
648 Chemistry Fundamentals. 1976; 15(1): 92-94.

649 [34]Chen M, Xie Y, Wu H, Shi S, Yu J. Modeling solubility of nitrogen in clean fire
650 extinguishing agent by Peng-Robinson equation of state and a correlation of Henry's law
651 constants. Appl Therm Eng. 2016; 110: 457-468.

652 [35]Holden BS, Katz JL. The homogeneous nucleation of bubbles in superheated binary liquid
653 mixtures. AIChE J. 1978; 24(2): 260-267.

654 [36]Lepori L, Gianni P, Matteoli E. Thermodynamic study of tetrachloromethane or heptane +
655 cycloalkane mixtures. J Therm Anal Calorim. 2016; 124: 1497-1509.

656 [37]Matteoli E, Lepori L, Porcedda S. Thermodynamic study of mixtures containing
657 dibromomethane. J Therm Anal Calorim. 2018; 132: 611-621.

658 [38]Chen M, Xie Y, Guo X, Yu J, Ma W. Predicting filling mass of nitrogen in fire agent bottle
659 based on Peng-Robinson equation of state with Wong-Sandler mixing rule. Journal of
660 Beijing University of Aeronautics and Astronautics (in Chinese). 2016; 42(10): 2162-2167.

661 [39] Simoiu L, Trandafir I, Popescu G. New Thermodynamic Consistency Test for Isobaric
662 Vapour-Liquid Equilibrium Data. *J Therm Anal Calorim.* 1998; 52: 1023–1035.